

CrossMark
click for updatesCite this: *RSC Adv.*, 2015, 5, 74802Received 21st July 2015
Accepted 27th August 2015

DOI: 10.1039/c5ra14382a

www.rsc.org/advances

Lamellar Ni/Al-SBA-15 fibers: preparation, characterization, and applications as highly efficient catalysts for amine and imine syntheses

Ren Ren and Jiantai Ma*

A novel Ni/Al-SBA-15 fiber catalyst with a lamellar structure was prepared by the urea precipitation method and successfully utilized in the environmental-friendly reduction of nitro functionality. The applications of the catalyst in highly efficient one-pot amine and imine syntheses were developed; the physicochemical properties of the samples were evaluated with ICP-OES, N₂ adsorption, XRD, HRTEM, and EDX. This new catalyst highlights potent catalytic activities and a simple recycling process as an important environmentally-friendly feature.

Introduction

Al-SBA-15 mesoporous materials have been used as support materials for Ni-based catalysts due to their excellent properties, including high surface areas, large pore volumes, suitable acidity, ordered hexagonal pore arrays with pore diameters between 2 and 30 nm, and high hydrothermal and thermal stabilities. These unique features have made Al-SBA-15 materials of great industrial interest, particularly in moderate acid-catalyzed reactions^{1–13} in the areas of petroleum processing and fine chemicals production. As a result, the preparation and application of Al-SBA-15 materials have become very popular research topics.

It is important to control the particle size and dispersion of the metal particles, since these properties have shown great influence on the catalyst activity, selectivity, and lifetime.^{14–19} Two of the common methods to deposit active nickels are ion exchange and impregnation. Ion exchange generates highly dispersed catalysts but suffers from limited metal loads due to the support exchange capacity restriction. In contrast, poorly dispersed catalysts with high nickel loads are generally resulted from the impregnation method, thanks to the weak metal-support interaction. As a result, new synthetic methods with both excellent nickel loads and dispersion have become crucial for further catalyst development. To date, several attempts have been reported,^{20–26} particularly the deposition-precipitation method (DP).^{27–41} This method has been successfully applied in the preparation of various nickel catalysts.^{42–48} Compared with the products of the impregnation method, the catalysts

prepared by DP exhibit much smaller particle size and higher catalytic activities.

Despite the significant advantages of the DP methods, interestingly, up to now very few Ni/Al-SBA-15 catalysts prepared by the DP method have been reported. In this paper, we reported the utilization of the DP method for the development of a special morphology Ni/Al-SBA-15 catalyst with high dispersion, narrow particle distribution, and excellent thermal stability. This catalyst combined the merits of Al-SBA-15 as mesoporous acidic carrier and the advantages of nickel catalyst by urea precipitation. To our best knowledge, our studies were the first application of this catalyst in one pot syntheses of amines and imines. In addition, our catalytic system was highly efficient and environmental-friendly, which made it further promising industrial applications in future.

Experimental section

Preparation of Al-SBA-15

In a typical synthesis, 3 g P123 was dissolved in 70 mL water, and then 45 mL 4 mol L^{−1} HCl solution was added and stirred for 0.5 h at room temperature. After adding a calculated amount of Al(NO₃)₃·9H₂O and 6.45 g TEOS, the resulting solution was stirred at 40 °C for 20 h and then transferred into a polytetrafluoroethylene bottle and aged at 100 °C for 48 h. The product was filtered, washed, dried at 373 K overnight, and then calcined in air from room temperature to 823 K (1 K min^{−1}, 6 h at 823 K).

Preparation of Ni/Al-SBA-15 catalyst

The Ni/Al-SBA-15 catalyst was synthesized by the deposition-precipitation method using Al-SBA-15 as the support and nickel nitrate as the metallic precursor. 19.2 g Al-SBA-15 and 14.3 g Ni(NO₃)₂·6H₂O were dissolved in 300 mL water and stirred for

State Key Laboratory of Applied Organic Chemistry, Gansu Provincial Engineering Laboratory for Chemical Catalysis, College of Chemistry and Chemical Engineering, Lanzhou University, Lanzhou, 730000, PR China. E-mail: majiantai@lzu.edu.cn; Fax: +86 931 8912577

10 minutes, followed by addition of 9.8 g urea and stirred for 30 min. After heated to 333 K and stirred for 2 h, the resulting mixture was heated to 363 K over 5 h. The reaction product was filtered, washed three times with deionized water, dried at 373 K overnight and then calcined in air from room temperature to 823 K (1 K min^{-1} , 6 h at 823 K).

Characterization of the catalyst

The Al and Ni content of the catalyst were determined by inductively coupled plasma optical emission spectroscopy (ICP-OES). Measurements were performed on a Spectro CIROS CCD spectrometer. The X-ray diffraction (XRD) measurements were carried out on a Bruker AXS-D8 Advance powder diffractometer, using $\text{CuK}\alpha$ radiation (40 kV, 30 mA), with a scanning speed of $0.0057^\circ\text{ min}^{-1}$ in the range of $0.5^\circ \leq 2\theta \leq 8^\circ$ and $0.01^\circ\text{ min}^{-1}$ in the range of $5^\circ \leq 2\theta \leq 70^\circ$. Nitrogen sorption isotherms were measured at -196°C on a Micromeritics Tristar 3000 system in static measurement mode. The samples were outgassed at 150°C for 3 h prior to the sorption measurements. The Brunauer–Emmett–Teller (BET) equation was used to calculate the specific surface area from the adsorption data obtained. The pore volume and pore size distribution were calculated by the Barrett–Joyner–Halenda (BJH) method on the adsorption branch of the isotherm. The high resolution HRTEM images were obtained on a FEITecni G2 transmission electron microscope operated at 200 kV (FEI company). Elemental composition data were collected by energy dispersive X-ray spectroscopy (EDS) performed on a Tecni G2 microscope.

General procedure for reduction of nitro containing compounds and one-pot synthesis of imines

The reactions were carried out in a 100 mL stainless steel reactor equipped with a magnetic stirrer. In a typical reaction procedure, 1.0 mmol nitro containing compound (or 1.0 mmol nitro compound, 1.2 mmol aldehyde) and 15 mL ethanol were mixed with 15 mg Ni/Al-SBA-15 catalyst (and co-catalyst). The Ni load was about 12 wt%. Biphenyl was used as the internal standard. The reactor was flushed three times with H_2 at 0.5 MPa and adjusted to the desired pressure. The reacting mixture was heated to the desired temperature with stirring. After reaction was complete, the reactor was cooled by an ice-water bath and then slowly depressurized. The catalyst product was separated, the reaction conversion rate was analyzed by GC (P.E. Autosystem XL), and the product was confirmed by GC-MS (Agilent 6890N/5973N).

Results and discussion

Small angle XRD patterns

Powder X-ray diffraction (XRD) was employed to assess the structural ordering. XRD small-angle spectra of Ni/Al-SBA-15 and Al-SBA-15 are shown in Fig. 1. Although the position of the diffraction peaks slightly changed from sample to sample, obviously all mesoporous materials exhibited three well-resolved peaks related to (100), (110), and (200) planes. These diffraction lines were associated with long-range 2D hexagonal

ordering in the $P6mm$ space group. These results were consistent with the data reported by Zhao^{49,50} for SBA-15. Although the intensity of characteristic peaks of Ni/Al-SBA-15 decreased slightly as compared with Al-SBA-15 zeolite, but the difference of the position was not significant. This indicated that the hexagonal pore arrangement of the support was not obviously destroyed during the deposition–precipitation of Ni. Additionally, with the increase of the Ni load, the intensity of (100), (110) and (200) diffraction peaks obviously decreased. Based on the report of Park,⁵¹ this probably because the fact that along with the increase of the Ni load, NiO number deposited in the channel increased, which reduced the scattering intensity of amorphous pore walls. It suggested that NiO nanoparticles were mainly distributed in the channels of mesoporous molecular sieves.

Large angle XRD patterns

The powder XRD patterns in the high angle region of $5^\circ \leq 2\theta \leq 70^\circ$ for the samples were shown in Fig. 2. For all samples, the broad peak at $15^\circ\text{--}30^\circ$ was ascribed to amorphous silica.^{52,53} The samples 12% Ni/Al-SBA-15 showed two marked diffraction peaks in the 2θ of 37.3° and 62.9° , which corresponded to nickel oxide. The result was consistent with the related reports in characterizations.^{54–58} On the other hand, the nickel oxide diffraction peak was not present until 12 wt% Ni was added, indicating that the Ni species were highly dispersed on the catalysts.

N_2 adsorption–desorption studies

N_2 adsorption/desorption isotherms and pore size distributions were presented in Fig. 3 and 4. The isotherms allowed calculation of specific surface area, pore volume, pore size distribution *etc.* Furthermore, the position and shape of hysteresis loop also provided useful information about the shape and size of the pores. The isotherms (Fig. 3) were typical type IV with an H1 hysteresis loop, which was a typical adsorption for mesoporous materials with 2D-hexagonal structure, similar to mesoporous siliceous SBA-15.^{59,60} The initial increase in adsorption capacity at low relative pressure was due to monolayer adsorption on mesopores. The upward deviation in the range of P/P_0 0.4–0.9

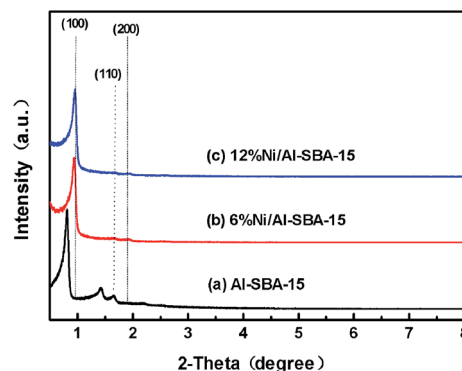


Fig. 1 Low angle XRD patterns of (a) Al-SBA-15, (b) 6% Ni/Al-SBA-15, (c) 12% Ni/Al-SBA-15.

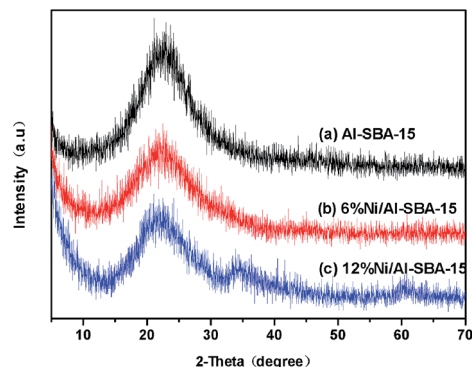


Fig. 2 Large angle XRD patterns of (a) Al-SBA-15, (b) 6% Ni/Al-SBA-15, (c) 12% Ni/Al-SBA-15.

was associated with progressive filling of mesopores. As the relative pressure increased all isotherms displayed a sharp increase characteristic of capillary condensation inside uniform mesopores, which were in agreement with the XRD results. Hysteresis loop was parallel, indicating a narrow and uniform pore size distribution. Compared with Al-SBA-15, P/P_0 of 12% Ni/Al-SBA-15 shifted to low values, because some Ni species were deposited on the pore surface, resulting the pore size reduction. With the increase of the Ni content, adsorption and desorption hysteresis area decreased.

The textural properties of all samples were presented in Table 1. With the nickel load increase, both the surface area and pore volume of samples decreased relatively. Al-SBA-15 exhibited larger surface areas ($505.1 \text{ m}^2 \text{ g}^{-1}$) and pore volume ($0.95 \text{ cm}^3 \text{ g}^{-1}$) than those of 12% Ni/Al-SBA-15.

Meanwhile, the average pore size increased with introduction of Ni on Al-SBA-15, from 7.77 to 10.82 nm (Fig. 4), which suggested that large amount of areas damaged parts pore when roasting.

HRTEM analysis and EDX

It is well known that the excellent structural ordering of the mesoporous materials can be directly observed by transmission electron microscopy. Fig. 5 showed representative HRTEM

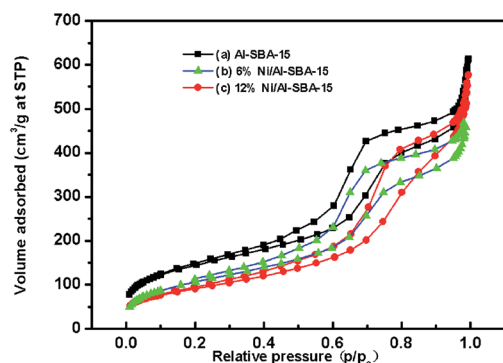


Fig. 3 Nitrogen adsorption/desorption isotherms of (a) Al-SBA-15, (b) 6% Ni/Al-SBA-15, (c) 12% Ni/Al-SBA-15.

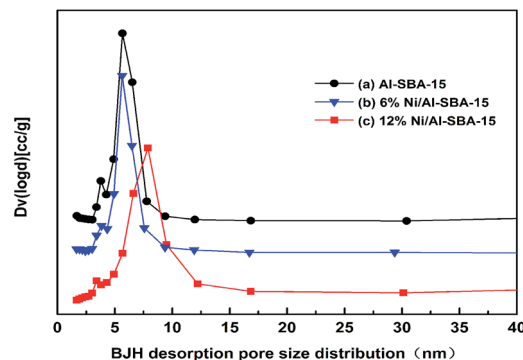


Fig. 4 Pore size distribution curves of (a) Al-SBA-15, (b) 6% Ni/Al-SBA-15, (c) 12% Ni/Al-SBA-15.

Table 1 Textural properties of the samples

Sample	BET ($\text{m}^2 \text{ g}^{-1}$)	Vp ($\text{cm}^3 \text{ g}^{-1}$)	Dp (nm)
12% Ni/Al-SBA-15	327.1	0.89	10.82
6% Ni/Al-SBA-15	389.4	0.86	8.76
Al-SBA-15	505.1	0.95	7.77

images in the direction perpendicular to the pore axis of Ni/Al-SBA-15 material. Al-SBA-15 exhibited uniform mesoporous channels with 2D-hexagonal symmetry ($P_6 \text{ mm}$). To our surprise, Ni/Al-SBA-15 exhibited the beautiful lamellar fibrous structures (or flocculent structure). The particle exhibited straight, parallel and uniform channels with regular intervals, confirming that the one-dimensional long-range ordering of Al-SBA-15 was retained even after the incorporation of Ni species into the framework. The average pore diameter was 7.68 nm, which was similar to the results of N_2 adsorption/desorption isotherms.

Fig. 6 showed the TEM-EDX images of the 12% Ni/Al-SBA-15 catalyst. The composition of this sample was confirmed by the EDX spectrum, which revealed that Ni, Al, O, and Si were

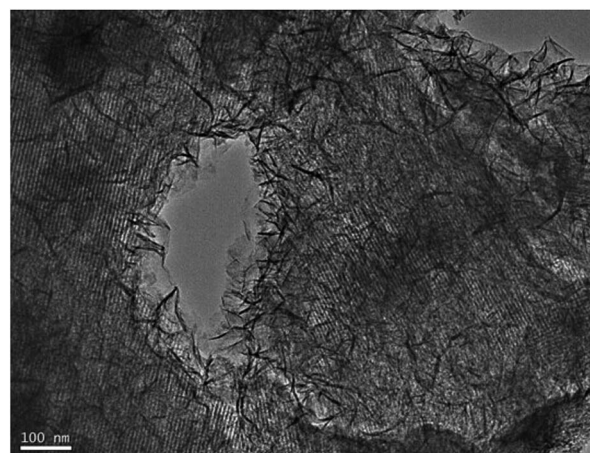


Fig. 5 HRTEM of 12% Ni/Al-SBA-15.

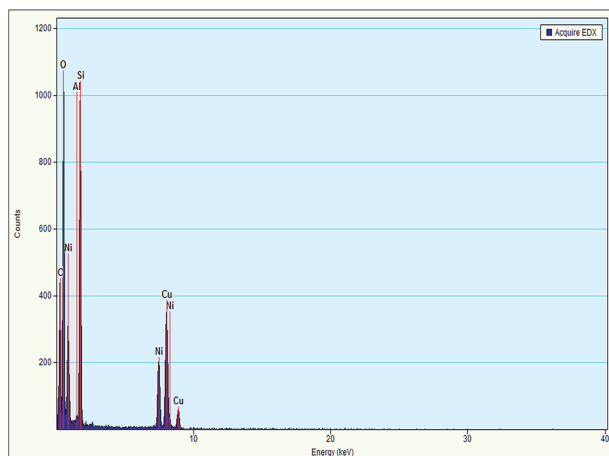


Fig. 6 EDX of 12% Ni/Al-SBA-15.

predominant species. In addition, C and Cu elements were also detected.

Synthesis of amines with the novel Ni/Al-SBA-15 catalyst

Amines are important intermediates in the chemistry of pharmaceuticals, dyes, pesticides and *etc.*^{64–87} Although different reagents and conditions have been investigated for the reduction of aromatic nitro compounds, most of these reductions have been associated with drawbacks such as harsh reaction conditions, use of expensive catalysts, formation of undesirable products, requirement of an excess amount of solvents, low yields, and *etc.* Additionally, very little attention has been paid to aliphatic nitro compounds as the substrates.^{88–90} For the increasing environmental and economic concerns, it is now necessary for chemists to develop environment-friendly reactions for traditional chemical transformations. Therefore, we tested our Ni/Al-SBA-15 catalyst in the reduction of nitro-containing compounds for the preparation of various amines.

As shown in Table 2, aliphatic amines (entries 1–6) were obtained in near quantitative yields in all cases, confirming that under these conditions aliphatic nitro compounds and the product amines were compatible with Ni/Al-SBA-15. To our relief, chain length and steric effect did not have much impact on the formation of amines. Excellent yields of the aliphatic amine formations (entries 1–6) were obtained. In addition, the catalyst exhibited excellent selectivity, nitro group was reduced while the C=C double bond was stable under the reaction conditions (entry 4). And dechlorination was minimal (entry 6) in our case.

The reaction results of aromatic nitro compounds (entries 7–11) were also shown in Table 2. We were delight to find that our catalyst reduced a wide variety of nitro compounds smoothly and efficiently. Slight dechlorination was observed in entry 8. The dinitro compound (entry 9) was also reduced with a high conversion and yield, and this result is better than previous work.⁶⁴ A slightly lower yield (80%) was obtained in entry 10, in part due to the harsh experiment conditions leading to the over-reduction of the ketone.

Table 2 Reduction of aliphatic and aromatic nitro compounds^a

$\text{R-NO}_2 \xrightarrow[\text{H}_2, \text{ethanol}]{\text{Ni/Al-SBA-15}} \text{R-NH}_2$				
Entry	Substrate	Product	Con. (%)	Yield ^b (%)
1			100	>99
2			100	>99
3			100	>99
4			100	>99
5			100	>99
6			100	97
7			100	>99
8			100	95
9			100	>99
10			100	80
11			100	>99

^a Reaction conditions: 1.0 mmol nitro compounds, 15 mL ethanol, 15 mg 12% Ni/Al-SBA-15, 383 K, 2.5 MPa H₂, 7.5 h. ^b GC yields.

One pot synthesis of imines with the novel Ni/Al-SBA-15 catalyst

Imines, also known as the Schiff base, are important nitrogen sources and key intermediates in different types of reactions utilized in biological, pharmaceutical, and industrial chemical synthesis.^{91–106} Traditional formation of imines from nitroarenes requires two separate steps in which the nitroarene is first reduced to the aniline, then isolated and subsequently condensed with the desired carbonyl-containing compound.^{107–122} As an alternative, catalytic one pot systems for imine synthesis have been under investigations. Several catalysts including Rh₆(CO)₁₆,¹¹³ PdCl₂-(PPh₃)₂/SnCl₂/CO,¹¹⁴ Pd/C/H₂,⁹⁶ and Ru₃(CO)₁₂/CO¹¹⁵ have been reported. However, severe drawbacks still remain and challenges have not yet been effectively met. For example, these protocols normally require noble metal catalysts, large excess amounts of oxidants, elevated pressures, high temperatures, which made them far from practical for large scale synthetic purposes. Thus, the development of efficient, environmental-friendly, and atom-economical syntheses of imines has become a very popular research field. Recently one pot synthesis was suggested as a promising solution,^{116–122} but the synthesis of imines using amine and alcohol as the feedstock in most cases. Masazumi Tamura reported the direct synthesis of imines from alcohols and amines over CeO₂ at low temperatures,¹¹⁶ Zhi-Xiang Wang developed selective imine formations from alcohols and amines catalyzed by the ruthenium(II)-PNP pincer complex,¹¹⁷ Taylor described a tandem oxidation-imine formation process from alcohols with

active manganese oxide,¹¹⁹ Jaiwook Park reported one-pot synthesis of imines and secondary amines by Pd-catalyzed coupling of benzyl alcohols and primary amines,¹²⁰ Sithambaram reported direct catalytic synthesis of imines from alcohols using manganese octahedral molecular sieves.⁹⁷

To the best of our knowledge, one-pot syntheses of imines directly from nitro compounds and aldehydes were rare.^{91,123} In this paper, we reported an efficient and environment-friendly one-pot synthetic route for imine formations using nitro compounds and aldehydes as the feedstock. The amine intermediates were provided *in situ* by the Ni/Al-SBA-15 catalyzed reduction of the nitro-containing substrates, which without work-up, were condensed with aldehydes to yield amins. Upon the subsequent dehydration, the desired imines were obtained in excellent yields.

Synthesis imines with different catalyst systems

The efficacy of Ni/Al-SBA-15 for nitrobenzene reduction–condensation reactions was compared with a number of catalyst systems (Table 3). The 12% Ni/Al-SBA-15 catalyst exhibited the highest activity (no. 1–15). Other metal catalysts such as 7.5% Ru/C, 10% Pd/C, and 10% RANEY® nickel were found to be feeble under the same conditions (no. 7–15).

When Pd/C was used (no. 11–14), no desired imine was obtained (only benzyl alcohol, aniline, and *N*-benzylaniline were produced), which was basically consistent with the previous reports.⁹¹ Under the conditions (no. 9 and 10), some desired imine products were generated with a slightly low conversions and selectivities. Al-SBA-15 was found to be a good co-catalyst, which could serve as a Lewis acid in the imine formation (no. 9 and 10). RANEY® nickel was pyrophoric and did not show any

chemoselectivity towards functional groups, such as C=O and NO₂ (no. 15).

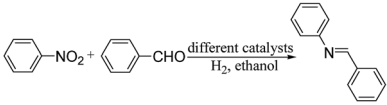
In addition, effects of various common solvents were investigated (Table 3). C₂H₅OH proved to be the best. Toluene, as a non-polar and aprotic solvent, gave 92.54% conversion and 94.56% selectivity. CH₂Cl₂ and CH₃OH, also promoted this catalytic reaction with less efficiency. H₂O led to a substantially low yield. In our experiments later on, only ethanol was chosen based on requirements of “green chemistry”, since ethanol can easily be generated from renewable sources and available all over the world.

The one pot synthesis of imines with the Ni/Al-SBA-15 catalyst directly from nitro compounds and aldehydes was speculated to have two major steps: reduction of nitro group to amine and subsequent condensation with aldehydes with the water removal facilitated by the catalyst. Moreover, in order to further determine the role of Al-SBA-15 in the imine formation, we screened the reaction of benzaldehyde with aniline in the presence and absence of Al-SBA-15 (RT, 0.1 Mpa, 1 h). Without Al-SBA-15 was used, the desired product was obtained in a 57% yield while using Al-SBA-15 improved the reaction yield to 97%. The results confirmed that Al-SBA-15 was an effective co-catalyst in the imine formation.

One-pot reduction–condensation reactions

The optimized conditions were then applied to more nitro compounds and aldehydes to extend the scope of the method. As shown in Table 4 (entries 12 and 13), imine formations from aliphatic nitro compounds and benzaldehyde have been investigated. A wide range of nitro compounds were tested with the Ni/Al-SBA-15 catalyst under the optimized conditions and almost all desired transformations were achieved with excellent conversion and in satisfactory yields.

Table 3 Comparison of catalytic activities with different catalytic systems^a



No.	Catalyst	Co-catalyst	Solvent	Time (h)	Pres. (Mpa)	Temp. (K)	Con. ^b	Sel. ^c
1	12% Ni/Al-SBA-15	—	C ₂ H ₅ OH	8	1.4	378	98.54	99.47
2	12% Ni/Al-SBA-15	—	CH ₃ OH	8	1.4	378	98.92	98.87
3	12% Ni/Al-SBA-15	—	CH ₂ Cl ₂	8	1.4	378	90.12	92.17
4	12% Ni/Al-SBA-15	—	Toluene	8	1.4	378	92.54	94.56
5	12% Ni/Al-SBA-15	—	H ₂ O	8	1.4	378	35.31	93.54
6	12% Ni/SBA-15	—	C ₂ H ₅ OH	8	1.4	378	98.57	89.42
7	7.5% Ru/C	—	C ₂ H ₅ OH	8	0.1	298	0	0
8	7.5% Ru/C	—	C ₂ H ₅ OH	8	1.4	323	0	0
9	7.5% Ru/C	—	C ₂ H ₅ OH	8	1.4	378	25.79	79.67
10	7.5% Ru/C	Al-SBA-15	C ₂ H ₅ OH	8	1.4	378	34.67	79.34
11	10% Pd/C	Al-SBA-15	C ₂ H ₅ OH	8	1.4	378	100	0
12	10% Pd/C	—	C ₂ H ₅ OH	8	1.4	378	100	0
13	10% Pd/C	Al-SBA-15	C ₂ H ₅ OH	8	1.4	298	100	0
14	10% Pd/C	—	C ₂ H ₅ OH	6	0.1	298	100	0.26
15	10% RANEY® nickel	—	C ₂ H ₅ OH	1	0.1	298	100	0.16

^a Reaction condition: 1.0 mmol nitrobenzene, 1.2 mmol benzaldehyde, 15 mL solvent, 15 mg catalyst, 3 mg co-catalyst. ^b Conversion of nitrobenzene. ^c Selectivity to imine.

As shown in Table 4 (entries 14–19), imine formations from aromatic nitro compounds and a variety of aldehydes have been investigated too. A series of aromatic aldehydes were utilized and all imines were obtained in excellent conversion and yields, which demonstrated the method possessed excellent functional group tolerance.

Interestingly, while electronic effects from the substituents on both nitroarenes and aromatic aldehydes had little influence on the overall reaction yields, steric hinderance around the nitro group seemed to play an important role in the imine formations (entries 17–19), with the decreasing of steric effect, the yields increased.

Proposed reaction mechanism

Imine synthesis proceeded *via* two mechanistically distinct reaction steps promoted by a single Ni catalyst (Ni/Al-SBA-15). Possible mechanistic studies of the reaction were also illustrated in Scheme 1. The first step was the reduction of the nitro compounds to the corresponding amines. The second step involved a nucleophilic attack on the aldehyde carbonyl group by the *in situ* generated amines. Ni/Al-SBA-15 provides Lewis acidic sites for hydrogen in order to facilitate the catalytic imine formation.

Imine synthesis is generally a facile reaction due to the good electrophilic properties of carbonyls and nucleophilic properties of the amine groups; however, for imines which are difficult to synthesize due to the decrease in electrophilicity/nucleophilicity of the carbonyl/amine groups a catalyst such as Ni/Al-SBA-15 is required.

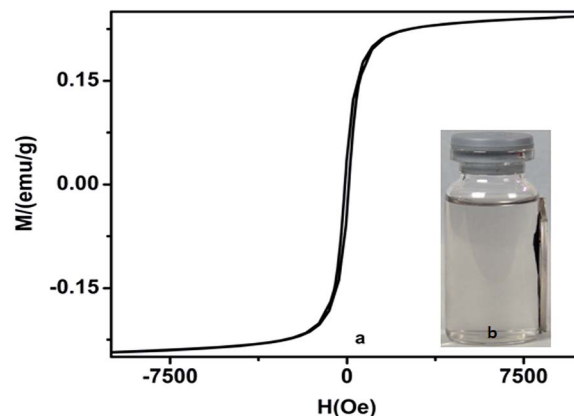


Fig. 7 (a) Hysteresis curves; (b) magnetic separation.

Catalyst regeneration and stability

The Ni/Al-SBA-15 catalyst displayed superparamagnetic behavior and no remanence at room temperature in Fig. 7a.

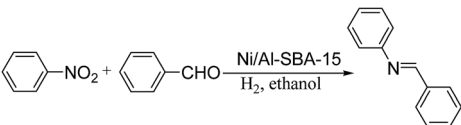
These indicated our Ni/Al-SBA-15 catalyst can be easily recovered and reused. In Fig. 7b, the Ni/Al-SBA-15 catalyst showed strong magnetism, as a result, it can simply be separated from reaction mixture in a relatively low magnetic field with a small laboratory magnet and recovered quantitatively by simple filtration. Regeneration of the catalyst was achieved by rinsing with ethanol. More interestingly, after magnetic recovery, the catalyst can be dispersed ready for further use.

Table 4 One-pot reduction–condensation reactions of aliphatic and aromatic nitro compounds^a

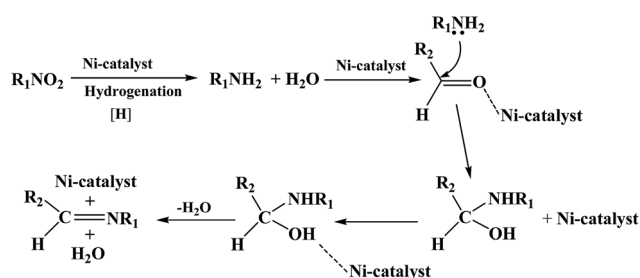
$\text{R}_1\text{-NO}_2 + \text{R}_2\text{-CHO} \xrightarrow[\text{H}_2, \text{ethanol}]{\text{Ni/Al-SBA-15}} \text{R}_1\text{-N=C-R}_2$					
Entry	Substrate	By-substrate	Product	Con. (%)	Yield ^b (%)
12				100	99
13				100	99
14				99	98
15				100	99
16				100	73
17				95	84
18				96	89
19				98	91

^a Reaction conditions: 1.0 mmol nitro compounds, 1.2 mmol aldehydes, 15 mL ethanol, 15 mg Ni/Al-SBA-15, 378 K, 1.4 MPa H₂, 8 h. ^b GC yields.

Table 5 Ni/Al-SBA-15 catalyst recycling experiments^a

				
Cycle no.	1 st	2 nd	3 rd	4 th
Yield ^b (%)	98	98	97	95

^a Reaction condition: 1.0 mmol nitrobenzene, 1.2 mmol benzaldehyde, 15 mL ethanol, 15 mg Ni/Al-SBA-15, 378 K, 1.4 MPa H₂, 8 h. ^b GC yields.



Scheme 1 The proposed mechanism for the one pot imine synthesis.

Nickel leaching of the catalyst was also studied. The Ni loading of the regenerated catalyst (after four cycles) was about 11.6 wt% (slightly lower than the fresh catalyst) and no obvious leaching of the catalyst occurred under our reaction conditions.

For practical applications of heterogeneous systems, the lifetime of the catalyst and its reusability are two important concerns. To clarify this issue, we established a series of experiments using the recycled Ni/Al-SBA-15 catalyst. To our satisfaction, the results demonstrated only slight decrease in the reaction yield (Table 5) after four recycles. In addition, the ease of catalyst reuse provided our catalyst significant advantages over commercial RANEY® nickel catalysts.

Conclusions

In this work, a novel and potent Ni/Al-SBA-15 catalyst was prepared and successfully applied in the environment-friendly reduction of nitro-containing compounds and the synthesis of imines by the one-pot reduction–condensation sequence. In addition, the catalyst was able to maintain high catalytic reactivity after multiple recycles and can easily be isolated and regenerated. These interesting features suggested that our catalyst had good prospects for further industrial applications and large-scale green production of imines and amines.

Acknowledgements

This research was supported by the Fundamental Research Funds for the Central Universities (grant no. lzujbky-2013-234 and 861605).

Notes and references

- W. Hu, Q. Luo, Y. Su, L. Chen, Y. Yue, C. Ye and F. Deng, *Microporous Mesoporous Mater.*, 2006, **92**, 22–30.
- A. J. J. Koekkoek, J. A. Rob van Veen, P. B. Gerretsen, P. Giltay, P. C. M. M. Magusin and E. J. M. Hensen, *Microporous Mesoporous Mater.*, 2012, **151**, 34–43.
- G. M. Kumaran, S. Garg, K. Soni, M. Kumar, J. K. G. D. Sharma, K. S. R. Rao and G. M. Dhar, *Microporous Mesoporous Mater.*, 2008, **114**, 103–109.
- R. V. Grieken, J. M. Escola, J. Moreno and R. Rodriguez, *Appl. Catal., A*, 2006, **305**, 176–188.
- H. Wang, Y. Liu and T. J. Pinnavaia, *J. Phys. Chem. B*, 2006, **110**, 4524–4526.
- K. S. Triantafyllidis, A. A. Lappas, I. A. Vasalos, H. Wang, Y. Liu and T. J. Pinnavaia, *Catal. Today*, 2006, **112**, 33–36.
- S. Zeng, J. Blanchard, M. Breyse, Y. Shi, X. Shu, H. Nie and D. Li, *Microporous Mesoporous Mater.*, 2005, **85**, 297–304.
- C. Nie, L. Huang, D. Zhao and Q. Li, *Catal. Lett.*, 2001, **71**, 117–125.
- T. Sano, T. Nijmi, T. Miyazaki, S. Tsubaki, Y. Oumi and T. Uozumi, *Catal. Lett.*, 2001, **71**, 105–110.
- Y. Xia and R. Mokaya, *J. Mater. Chem.*, 2004, **14**, 3427–3435.
- J. M. Rosenholm, T. Czuryzkiewicz, F. Kleitz, J. B. Rosenholm and M. Linden, *Langmuir*, 2007, **23**, 4315–4323.
- D. G. Poduval, J. A. R. van Veen, M. S. Rigutto and E. J. M. Hensen, *Chem. Commun.*, 2010, **46**, 3466–3468.
- E. J. M. Hensen, D. G. Poduval, D. A. J. M. Ligthart, J. A. R. van Veen and M. S. Rigutto, *J. Phys. Chem. C*, 2010, **114**, 8363–8374.
- P. Castellazzi, G. Groppi, P. Forzatti, A. Baylet, P. Marécot and D. L. Duprez, *Catal. Today*, 2010, **155**, 18–26.
- A. M. Banerjee, M. R. Pai, R. Tewari, N. Raje, A. K. Tripathi, S. R. Bharadwaj and D. Das, *Appl. Catal., B*, 2015, **162**, 327–337.
- R. M. M. Abbaslou, J. Soltan and A. K. Dalai, *Appl. Catal., A*, 2010, **379**, 129–134.
- R. M. Rioux, H. S. J. D. Hoefelmeyer, P. Yang and G. A. Somorjai, *J. Phys. Chem. B*, 2005, **109**, 2192–2202.
- I. O. Costilla, M. D. Sanchez and C. E. Gigola, *Appl. Catal., A*, 2014, **478**, 38–44.
- M. P. Casaleto, A. Longo, A. M. Venezia, A. Martorana and A. Prestianni, *Appl. Catal., A*, 2006, **302**, 309–316.
- Z. Wu, S. Ge, M. Zhang, W. Li and K. Tao, *J. Colloid Interface Sci.*, 2009, **330**, 359–366.
- X. Hao, Y. Zhang, J. Wang, W. Zhou, C. Zhang and S. Liu, *Microporous Mesoporous Mater.*, 2006, **88**, 38–47.
- Y. Kuang, Y. Cui, Y. Zhang, Y. Yu, X. Zhang and J. Chen, *Chem.–Eur. J.*, 2012, **18**, 1522–1527.
- M. Rana, Y. Liu, W. Chu, Z. Liu and A. Borgna, *Catal. Commun.*, 2012, **27**, 69–72.
- K. Song, H. Zhang, Y. Zhang, Y. Tang and K. Tang, *J. Catal.*, 2013, **299**, 119–128.
- R. Baran, I. I. Kaminska, A. Srebowata and S. Dzwigaj, *Microporous Mesoporous Mater.*, 2013, **169**, 120–127.

- 26 F. Menegazzo, M. Signoretto, G. Frison, F. Pinna, G. Strukul, M. Manzoli and F. Boccuzzi, *J. Catal.*, 2012, **290**, 143–150.
- 27 S. Chytil, W. R. Glomm and E. A. Blekkan, *Catal. Today*, 2009, **147**, 217–223.
- 28 E. Río, G. Blanco, S. Collins, M. L. Haro, X. Chen, J. J. Delgado, J. J. Calvino and S. Bernal, *Top. Catal.*, 2011, **54**, 931–940.
- 29 A. J. Binder, Z. Qiao, G. M. Veith and S. Dai, *Catal. Lett.*, 2013, **143**, 1339–1345.
- 30 E. Rio and M. L. Haro, *Chem. Commun.*, 2013, **49**, 6722–6724.
- 31 S. S. R. Putluru, L. Schill, S. Mossin, A. D. Jensen and R. Fehrmann, *Catal. Lett.*, 2014, **144**, 1170–1177.
- 32 A. Sandoval, C. Louis and R. Zanella, *Appl. Catal., B*, 2013, **140–141**, 363–377.
- 33 S. S. R. Putluru, L. Schill, A. D. Jensen, B. Siret, F. Tabaries and R. Fehrmann, *Appl. Catal., B*, 2015, **165**, 628–635.
- 34 H. Xu, W. Chu, J. Luo and M. Liu, *Catal. Commun.*, 2010, **11**, 812–815.
- 35 P. Miquel, P. Granger, N. Jagtap, S. Umbarkar, M. Dongare and C. Dujardin, *J. Mol. Catal. A: Chem.*, 2010, **322**, 90–97.
- 36 S. Ajaikumar, J. Ahlqvist, W. Larsson, A. Shchukarev, A. R. Leino, K. Kordas and J. P. Mikkola, *Appl. Catal., A*, 2011, **392**, 11–18.
- 37 S. Chytil, W. R. Glomm, I. Kvande, T. Zhao, J. C. Walmsley, E. A. Blekkan, *Top. Catal.*, 2007, **45**(1–4), 93–99.
- 38 X. Lu, G. Zhao and Y. Lu, *Catal. Sci. Technol.*, 2013, **3**, 2906–2909.
- 39 S. S. R. Putluru, L. Schill, D. Gardini, S. Mossin, J. B. Wagner, A. D. Jensen and R. Fehrmann, *J. Mater. Sci.*, 2014, **49**, 2705–2713.
- 40 F. Zhong, Y. Xiao, X. Weng, K. Wei, G. Cai, Y. Zheng and Q. Zheng, *Catal. Lett.*, 2009, **133**, 125–133.
- 41 K. Qian, J. Fang, W. Huang, B. He, Z. Jiang, Y. Ma and S. Wei, *J. Mol. Catal. A: Chem.*, 2010, **320**, 97–105.
- 42 M. K. van der Lee, A. Jos van Dillen, J. H. Bitter and K. P. de Jong, *J. Am. Chem. Soc.*, 2005, **127**, 13573–13582.
- 43 R. Gómez-Reynoso, J. Ramírez, R. Nares, R. Luna and F. Murrieta, *Catal. Today*, 2005, **107–108**, 926–932.
- 44 P. Burattin, M. Che and C. Louis, *J. Phys. Chem. B*, 2000, **104**, 10482.
- 45 R. Nares, J. Ramirez, A. Gutierrez, C. Louis and T. Klimova, *J. Phys. Chem. B*, 2002, **106**, 13287–13293.
- 46 R. Nares, *Ph.D. Thesis*, Unam, Mexico, 2003.
- 47 R. Nares, J. Ramirez, A. G. Alejandre and R. Cuevas, *Ind. Eng. Chem. Res.*, 2009, **48**, 1154–1162.
- 48 J. Cao, Z. Yan, Q. Deng, Z. Yuan, Y. Wang, G. Sun, X. Wang, B. Hari and Z. Zhang, *Catal. Sci. Technol.*, 2014, **4**, 361–368.
- 49 D. Zhao, J. Feng, Q. Huo, N. Melosh, G. H. Fredrickson, B. F. Chmelka and G. D. Stucky, *Science*, 1998, **279**, 548–552.
- 50 D. Zhao, Q. Huo and J. Feng, *J. Am. Chem. Soc.*, 1998, **120**, 6024–6036.
- 51 Y. Park, T. Kang and P. Kim, *J. Colloid Interface Sci.*, 2006, **295**, 464–471.
- 52 N. A. Dhas, A. Zaban and A. Gedanken, *Chem. Mater.*, 1999, **11**, 806–813.
- 53 H. Liu, H. Wang, J. Shen, Y. Sun and Z. Liu, *Appl. Catal., A*, 2008, **337**, 138–147.
- 54 D. J. Lensveld, G. MesuJ and A. J. Dillen, *Microporous Mesoporous Mater.*, 2001, **44–45**, 401–407.
- 55 M. A. Gondal, T. A. Saleh and Q. A. Drmosh, *Appl. Surf. Sci.*, 2012, **258**, 6982–6986.
- 56 K. V. R. Chary, P. V. R. Rao and V. V. Rao, *Catal. Commun.*, 2008, **9**, 886–893.
- 57 S. Ren, P. Zhang, H. Shui, Z. Lei, Z. Wang and S. Kang, *Catal. Commun.*, 2010, **12**, 132–136.
- 58 A. Albarazi, M. E. Galvez and P. D. Costa, *Catal. Commun.*, 2015, **59**, 108–112.
- 59 Z. Luan, M. Hartmann and D. Zhao, *Chem. Mater.*, 1999, **11**, 1621–1627.
- 60 Z. Luan, E. M. Maes and P. A. W. van der Heide, *Chem. Mater.*, 1999, **11**, 3680–3686.
- 61 S. Enthaler, *Catal. Lett.*, 2011, **141**, 55–61.
- 62 D. He, H. Shi, Y. Wu and B. Xu, *Green Chem.*, 2007, **9**, 849–851.
- 63 R. J. J. Rahaim and R. E. J. Maleczka, *Org. Lett.*, 2005, **7**, 5087–5090.
- 64 Y. Chen, J. Qiu, X. Wang and J. Xiu, *J. Catal.*, 2006, **242**, 227–230.
- 65 P. L. Gkizis, M. Stratakis and I. N. Lykakis, *Catal. Commun.*, 2013, **36**, 48–51.
- 66 Z. Zhao, H. Yang, Y. Li and X. Guo, *Green Chem.*, 2014, **16**, 1274–1281.
- 67 H. Göksua, H. Can, K. Sendil, M. S. Gültekina and Ö. Metina, *Appl. Catal., A*, 2014, **488**, 176–182.
- 68 F. Zamani and S. Kianpour, *Catal. Commun.*, 2014, **45**, 1–6.
- 69 U. Sharma, P. Kumar, N. Kumar, V. Kumar and B. Singh, *Adv. Synth. Catal.*, 2010, **352**, 1834–1840.
- 70 R. G. de Noronha, C. C. Romao and A. C. Fernandes, *J. Org. Chem.*, 2009, **74**, 6960–6964.
- 71 X. Lou, L. He, Y. Qian, Y. Liu, Y. Cao and K. Fan, *Adv. Synth. Catal.*, 2011, **353**, 281–286.
- 72 A. Saha and B. Ranu, *J. Org. Chem.*, 2008, **73**, 6867–6870.
- 73 D. Cantillo, M. M. Moghaddam and C. O. Kappe, *J. Org. Chem.*, 2013, **78**, 4530–4542.
- 74 M. L. Kantam, R. Chakravarti, U. Pal, B. Sreedhar and S. Bhargava, *Adv. Synth. Catal.*, 2008, **350**, 822–827.
- 75 S. Farhadi and F. Siadatnasab, *J. Mol. Catal. A: Chem.*, 2011, **339**, 108–116.
- 76 U. Sharma, P. K. Verma, N. Kumar, V. Kumar, M. Bala and B. Singh, *Chem.-Eur. J.*, 2011, **17**, 5903–5907.
- 77 P. Veerakumar, M. Velayudham, K. L. Lu and S. Rajagopal, *Appl. Catal., A*, 2012, **439–440**, 197–205.
- 78 H. Wang, J. Yan, W. Chang and Z. Zhang, *Catal. Commun.*, 2009, **10**, 989–994.
- 79 H. Min, S. Lee, M. Park, J. Hwang, H. Jung and S. Lee, *J. Organomet. Chem.*, 2014, **755**, 7–11.
- 80 I. Pogorelic, M. F. Litvic, S. Merkas, G. Ljubic, I. Cepanec and M. Litvi, *J. Mol. Catal. A: Chem.*, 2007, **274**, 202–207.
- 81 M. Baron, E. Métay, M. Lemaire and F. Popowycz, *Green Chem.*, 2013, **15**, 1006–1015.
- 82 D. Shah and H. Kaur, *J. Mol. Catal. A: Chem.*, 2014, **381**, 70–76.

- 83 R. K. Rai, A. Mahata, S. Mukhopadhyay, S. Gupta, P. Li, K. T. Nguyen, Y. Zhao, B. Pathak and S. K. Singh, *Inorg. Chem.*, 2014, **53**, 2904–2909.
- 84 R. J. Kalbasi, A. A. Nourbakhsh and F. Babaknezhad, *Catal. Commun.*, 2011, **12**, 955–960.
- 85 U. Sharma, N. Kumar, P. K. Verma, V. Kumar and B. Singh, *Green Chem.*, 2012, **14**, 2289–2293.
- 86 A. Corma, P. Concepcion and P. Serna, *Angew. Chem., Int. Ed.*, 2007, **46**, 7266–7269.
- 87 C. G. Morales-Guio, I. Yuranov and L. Kiwi-Minsker, *Top. Catal.*, 2014, **57**, 1526–1532.
- 88 A. Akita, M. Inbia, H. Uchida and A. Ohta, *Synthesis*, 1977, 792–794.
- 89 H. N. Borah, D. Prajapati, J. S. Sandhu and A. C. Ghosh, *Tetrahedron Lett.*, 1994, **35**, 3167–3170.
- 90 D. C. Gowda, B. Mahesh and S. Gowda, *Indian J. Chem., Sect. B: Org. Chem. Incl. Med. Chem.*, 2001, **40**, 75–77.
- 91 A. L. Korich and T. S. Hughes, *Synlett*, 2007, 2602–2604.
- 92 K. P. Guzen, A. S. Guarezemini, A. T. G. Orfao, R. Cella, C. M. P. Pereira and H. A. Stefani, *Tetrahedron Lett.*, 2007, **48**, 1845–1847.
- 93 L. L. Santos, P. Serna and A. Corma, *Chem.–Eur. J.*, 2009, **15**, 8196–8203.
- 94 H. Choi and M. P. Doyle, *Chem. Commun.*, 2007, 745–747.
- 95 S. Kegnæs, J. Mielby, U. V. Mentzel, C. H. Christensen and A. Riisager, *Green Chem.*, 2010, **12**, 1437–1441.
- 96 M. G. Banwell, D. W. Lupton, X. Ma, J. Renner and M. O. Sydnes, *Org. Lett.*, 2004, **6**, 2741–2744.
- 97 S. Sithambaram, R. Kumar, Y. Son and S. L. Suib, *J. Catal.*, 2008, **253**, 269–277.
- 98 A. Zanardi, J. A. Mata and E. Peris, *Chem.–Eur. J.*, 2010, **16**, 10502–10506.
- 99 H. A. Ho, K. Manna and A. D. Sadow, *Angew. Chem., Int. Ed.*, 2012, **51**, 8607–8610.
- 100 S. Murahashi, Y. Okano, H. Sato, T. Nakae and N. Komiya, *Synlett*, 2007, **11**, 1675–1678.
- 101 A. Simion, C. Simion, T. Kanda, S. Nagashima, Y. Mitoma, T. Yamada, K. Mimura and M. Tashiro, *J. Chem. Soc., Perkin Trans. 1*, 2001, 2071–2078.
- 102 N. E. Borisova, M. D. Reshetova and Y. A. Ustynyuk, *Chem. Rev.*, 2007, **107**, 46–79.
- 103 J. Barluenga, F. Aznar and C. Valdes, *Angew. Chem., Int. Ed.*, 2004, **43**, 343–345.
- 104 S. Guizzetti and M. Benaglia, *Eur. J. Org. Chem.*, 2010, 5529–5541.
- 105 A. Grirrane, A. Corma and H. Garcia, *J. Catal.*, 2009, **264**, 138–144.
- 106 V. Macho, M. Králik, J. Hudec and J. Cingelova, *J. Mol. Catal. A: Chem.*, 2004, **209**, 69–73.
- 107 K. Tanaka and R. Shiraishi, *Green Chem.*, 2000, **2**, 272–273.
- 108 K. P. Guzen, A. S. Guarezemini, A. T. G. Orfao, R. Cella, C. M. P. Pereira and H. A. Stefani, *Tetrahedron Lett.*, 2007, **48**, 1845–1848.
- 109 A. K. Chakraborti, S. Bhagat and S. Rudrawar, *Tetrahedron Lett.*, 2004, **45**, 7641–7644.
- 110 H. Naeimi, F. Salimi and K. Rabiei, *J. Mol. Catal. A: Chem.*, 2006, **260**, 100–104.
- 111 C. K. Z. Andrade, S. C. S. Takada, L. M. Alves, J. P. Rodrigues, P. A. Z. Suarez, R. F. Brandao and V. C. D. Soares, *Synlett*, 2004, **12**, 2135–2138.
- 112 M. Gopalakrishnan, P. Sureshkumar, V. Kanagarajan, J. Thanusu and R. Govindaraju, *J. Chem. Res.*, 2005, **5**, 299–303.
- 113 A. F. M. Iqbal, *J. Org. Chem.*, 1972, **37**, 2791–2795.
- 114 M. Akazome, T. Kondo and Y. Watanabe, *J. Org. Chem.*, 1994, **59**, 3375–3380.
- 115 M. Akazome, T. Kondo and Y. Watanabe, *J. Org. Chem.*, 1993, **58**, 310–312.
- 116 M. Tamura and K. Tomishige, *Angew. Chem., Int. Ed.*, 2015, **54**, 864–867.
- 117 H. Li, X. Wang, M. Wen and Z. Wang, *Eur. J. Inorg. Chem.*, 2012, 5011–5020.
- 118 H. Tian, X. Yu, Q. Li, J. Wang and Q. Xu, *Adv. Synth. Catal.*, 2012, **354**, 2671–2677.
- 119 L. Blackburn and R. J. K. Taylor, *Org. Lett.*, 2001, **3**, 1637–1639.
- 120 M. S. Kwon, S. Kim, S. Park, W. Bosco, R. K. Chidrala and J. Park, *J. Org. Chem.*, 2009, **74**, 2877–2879.
- 121 W. Cui, H. Zhu, M. Jia, W. Ao, Y. Zhang and B. Zhaorigetu, *React. Kinet., Mech. Catal.*, 2013, **109**, 551–562.
- 122 H. Sun, F. Su, J. Ni, Y. Cao, H. He and K. Fan, *Angew. Chem., Int. Ed.*, 2009, **48**, 4390–4393.
- 123 Y. Xiang, Q. Meng, X. Li and J. Wang, *Chem. Commun.*, 2010, **46**, 5918–5920.